NARROW BAND PHOTOMETRY OF COMET KOHOUTEK

Larry W. Brown

I. INTRODUCTION

Photometric observations of emission line features of the coma of comet Kohoutek (1973f) were made with narrow band interference filters. The emission features observed were CN(3879 A°), C_3(4057 A°), and C_2(4732, 5165,5634 A°). The radial dependence of the emission was investigated by employing six diaphragms set concentrically about the brightest part of the comet's head.

The photometric observations were made at the Optical Research Facility and Observatory of NASA/Goddard Space Flight Center (GSFC) in Greenbelt, Maryland. The observatory is located 13 miles Northeast of Washington, D.C. (longitude = $5^h07^m18^s.22$, latitude = +39° 01' 11".48, altitude = 49 meters) and is operated by the Laboratory for Optical Astronomy of Goddard (GSFC).

II. INSTRUMENTATION

The photoelectric measurements were made at the Cassegrain focus of a Boller and Chivens 36-inch telescope with a digital single channel pulse-counting system. This system consisted of an uncooled ITT model FW130 photomultiplier tube whose output was connected to a Lacroy preamplifier-discriminator followed by an Atec pulse counter. The output of the counter and the timing information were digitally recorded on a magnetic tape and processed by an IBM 360-91 computer. System timing was accomplished with a Tracor model 304D rubidium frequency standard.

https://doi.org/10.1017/S0252921100500761 Published online by Cambridge University Press

Table I
Filters

FILTER / PARAMETER	#4	#3	#9	#8	#7	#1	#6
ELEMENT	CN	C_3	C_2	C_2	Continuum	Visual	C_2
λ (A^o)	3879	4057	4732	5165	5200	5434	5634
$\Delta\lambda$ (A^o)	63	93	54	50	51	235	50
$\Delta\lambda$ (%)	1.6	2.3	1.1	1.0	1.0	4.3	0.9
Transmission (%)	42	58	75	75	83	61	87

The narrow band interference filters were manufactured by Thin Film, Inc. Tracings of each filter were made using a Carey model 14 spectrophotometer whose intensity scale was calibrated against a set of Balzer Incomel-coated neutral density filters. The results of these tracings are presented in Table I. The number assigned each filter represents its position in the filter holder. The parameters measured were the effective wavelength (λ), full width at half the maximum intensity ($\Delta\lambda$ in A^o and per cent λ), and the maximum transmission over the bandwidth.

III. OBSERVATIONS

The observations consisted of measurements with one wide and six narrow band filters. Five narrow band filters were chosen to correspond to the emission line features CN(3879 A^o), C_3(4057 A^o), C_2(4732, 5165, 5634 A^o) of the coma. The sixth narrow band filter was chosen to provide a reference continuum (5200 A^o) near the strongest C_2 emission band. The wide band filter represented an attempt to provide a bridge between the narrow band measurements and the visual magnitude of the UBVRI photometric system. In addition each filter was used with six diaphragm openings corresponding to 9,14,36,48,100 and 220 seconds of arc concentric circles about the brightest (visually) part of the comet's head.

The measurements were taken by selecting a filter,centering the brightest visual spot of the head in the smallest diaphragm, then recording

https://doi.org/10.1017/S0252921100500761 Published online by Cambridge University Press

a set of 30 data points of 1-second count intervals for each diaphragm from the smallest to the largest. The centering of the diaphragms was periodically checked; although, the variable drive setting of the telescope was found to compensate adequately for the motion of the comet. The data sets were averaged statistically in a computer to provide a 30 second count interval. This was done to provide some quality control over the data in an effort to compensate for the poor sky conditions near the horizon in the Washington metropolitan area. After a complete diaphragm sequence on the comet, the sequence was repeated on an area of sky. The comet measurements were then reduced by the appropriate sky measurements. Some care was taken to insure that these measurements were taken under as similiar a sky condition as those for the comet. This procedure was repeated for each of the filters. Normally the sequence followed that of the filter holder; however, when twilight interference was expected, the sequence was shifted so that those filters affected the most would be done in the darkest sky.

Whenever possible a reference star was observed both preceding and following the comet observation. The star was selected on the basis of its nearness to the comet position at the time of observation. Due to the spatially varying sky conditions, simultaneous spectral matching was not attempted in order to obtain the spatial match. The night's observing schedule was completed by similarly observing a number of other stars of different spectral type under different conditions of air mass and varying sky conditions. These stars were

https://doi.org/10.1017/S0252921100500761 Published online by Cambridge University Press

used to derive daily extinction corrections, to define a magnitude system corresponding to the narrow band filters used, and to check these parameters for consistency with the reference star - comet comparison.

IV. DATA REDUCTION

The raw data consists of a set of 30 data points of 1-second count intervals for each filter and diaphragm combination both on the comet and off (sky), and similarly, 60 data points both on and off the stars. These data were recorded on a 7-track magnetic tape for reduction on an IBM 360-91 computer. The initial step in the data reduction was to obtain the average 1-second pulse count and the standard deviation (σ) over the 30 or 60 second interval. Points which exceeded three times the standard deviation (3σ) were eliminated and new averages computed. If all the remaining points did not exceed the new 3σ level then the average was accepted. For those averages rejected, a visual inspection of data could in some cases eliminate bad sections of the interval and allow the recomputation of the average. The appropriate sky averages were then used to obtained the average pulse count above background for each measurement.

A least-squares-fit technique was applied to all star measurements for each particular day. This provided an approximate extinction correction for that day and a crudely defined magnitude scale. This initial fit showed that the photometric system scale was linear but that a small color correction was needed for the slope. Using the

https://doi.org/10.1017/S0252921100500761 Published online by Cambridge University Press

preliminary extinction corrections, all the daily measurements were combined to produce a more accurate magnitude scale. At this time obviously inconsistent star measurements were eliminated and the final daily extinction corrections and magnitude scale were computed. A total of 103 star measurements (Table II) were used in the final analysis. The daily extinction corrections and the average extinction are listed in Table III.

The magnitude scale is referenced to the UBVRI multicolor photometry system with magnitudes taken from the Arizona-Tonantzintla catalogue (Iriarte et al. 1965). The magnitudes for individual filters were found by fitting third degree polynomials to the UBVRI magnitudes (Table IV, Figure 1).

TABLE II

Reference Stars (UBVRI)

B.S.#	NAME	V	U-V	B-V	V-R	V-I	Mk SP	USED
875		$5^{m}.17$	0.13	0.08	0.11	0.18	A1 V	4
996	KAP CET	4.84	0.89	0.69	0.56	0.93	G5 V	20
1570	PI 1 ORI	4.66	0.16	0.08	0.11	0.14	A0 V	5
1983	GAM LEP	3.58	0.51	0.48	0.45	0.72	F6 V	3
2198	69 ORI	4.92	-0.71	-0.12	-0.02	-0.16	B5 V	4
2344	10 MON	5.04	-0.94	-0.18	-0.11	-0.27	B2 V	7
3492	RHO HYA	4.37	-0.10	-0.05	0.05	-0.02	A0 V	9
3759	TAU 1 HYA	4.60	0.46	0.45	0.40	0.63	F6 V	19
3970	UPS 2 HYA	4.58	-0.37	-0.09	-0.01	-0.09	B8 V	2
4119	BET SEX	5.09	-0.67	-0.13	-0.03	-0.18	B6 V	11
4468	THE CRT	4.70	-0.24	-0.08	0.03	-0.04	B9 V	6
8597	ETA AQR	4.00	-0.37	-0.09	-0.05	-0.12	B8 V	7
8969	IOT PSC	4.13	0.53	0.51	0.43	0.72	F7 V	6

TOTAL OBS. = 103

https://doi.org/10.1017/S0252921100500761 Published online by Cambridge University Press

TABLE III

Extinction

Filter / Day(J.D.)	#4	#3	#9	#8	#7	#1	#6
2441990.9	0^{m}59	0.55	0.39	0.32	0.31	0.28	0.26
2442010.0	0.56	0.52	0.38	0.33	0.33	0.31	0.30
2442016.9	0.59	0.55	0.39	0.31	0.30	0.27	0.24
2442018.0	0.62	0.59	0.46	0.38	0.38	0.33	0.29
2442021.0	0.59	0.55	0.39	0.31	0.30	0.27	0.24
2442060.5	0.59	0.55	0.39	0.31	0.30	0.27	0.24
2442061.5	0.63	0.55	0.33	0.22	0.22	0.17	0.14
2442069.5	0.69	0.61	0.34	0.20	0.19	0.13	0.09
2442075.5	0.53	0.50	0.38	0.30	0.30	0.25	0.22
2442080.6	0.78	0.73	0.56	0.47	0.47	0.43	0.41
2442094.6	0.66	0.60	0.40	0.30	0.29	0.24	0.22
2442096.6	0.61	0.54	0.31	0.19	0.18	0.12	0.08
2442099.6	0.64	0.57	0.33	0.21	0.21	0.15	0.12
Average	0^{m}59	0^{m}55	0^{m}39	0^{m}31	0^{m}30	0^{m}27	0^{m}24
	Range of Extinction Corrections to Data						
Minimum	1^{m}0	0^{m}9	0^{m}8	0^{m}6	0^{m}5	0^{m}4	0^{m}4
Maximum	3.6	3.6	1.6	1.4	1.5	2.3	1.4

TABLE IV

Reference Stars (UBVRI, 3rd Order Polynomial Fit)

Filter / Star	#4	#3	#9	#8	#7	#1	#6
B.S.#875	5^{m}28	5.27	5.22	5.19	5.18	5.17	5.15
996	5.70	5.64	5.27	4.99	4.97	4.81	4.70
1570	4.78	4.76	4.71	4.68	4.67	4.66	4.64
1983	4.13	4.11	3.90	3.69	3.68	3.55	3.47
2198	4.50	4.68	5.01	5.05	5.05	5.04	5.03
2344	4.52	4.66	4.92	4.93	4.93	4.92	4.90
3492	4.29	4.30	4.35	4.37	4.37	4.37	4.37
3759	5.11	5.10	4.90	4.71	4.69	4.58	4.50
3970	4.35	4.42	4.56	4.58	4.58	4.58	4.58
4119	4.70	4.83	5.07	5.10	5.10	5.09	5.08
4468	4.54	4.58	4.67	4.70	4.70	4.70	4.70
8597	3.78	3.84	3.98	4.00	4.00	4.00	4.00
8969	4.71	4.70	4.47	4.25	4.23	4.10	4.02

https://doi.org/10.1017/S0252921100500761 Published online by Cambridge University Press

Approximately 50% of the star measurements used to define the magnitude scale were on standard stars whose spectral characteristics (figure 2) have been measured with narrow band scanning photometers (Breger, 1971). These narrow band magnitudes (Table V) were compared to the UBVIR magnitudes. A correction factor for each filter's magnitude scale was obtained by averaging the individual difference for each standard star weighted by the number of observations of each star. The narrow band magnitude system was used then to obtain the observed magnitude of the comet. These magnitudes were found to be consistent with the direct comparisons made on the reference star measured preceeding and following the comet measurements.

TABLE V

Standard Stars (Normalized to 5480 A°)

Narrow Band System - Bandwidth ~50 A°

Star / Filter	#4	#3	#9	#8	#7	#1	#6
B.S.# 875	$0^m.56$	-0.14	-0.08	-0.02	-0.02	0.00	0.04
996				0.09	0.08	0.00	-0.04
1570	0.41	-0.20	-0.12	-0.06	-0.05	0.00	0.02
4119	-0.12	-0.44	-0.27	-0.12	-0.09	0.00	0.05
4468	0.22	-0.34	-0.18	-0.08	-0.07	0.00	0.03
8597	0.15	-0.31	-0.15	-0.06	-0.05	0.00	0.05
α LYR	0.45	-0.28	-0.15	-0.06	-0.05	0.00	0.04

https://doi.org/10.1017/S0252921100500761 Published online by Cambridge University Press

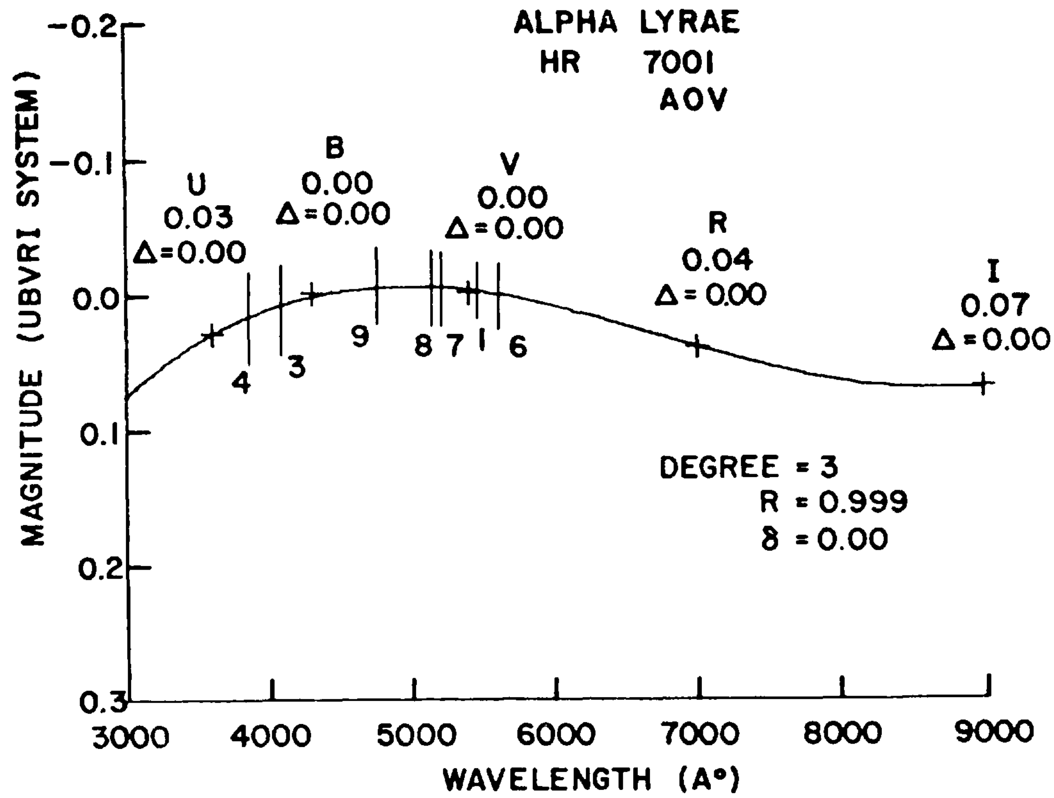

Figure 1 - Example of the determination of the star magnitude for each filter from the UBVRI system.

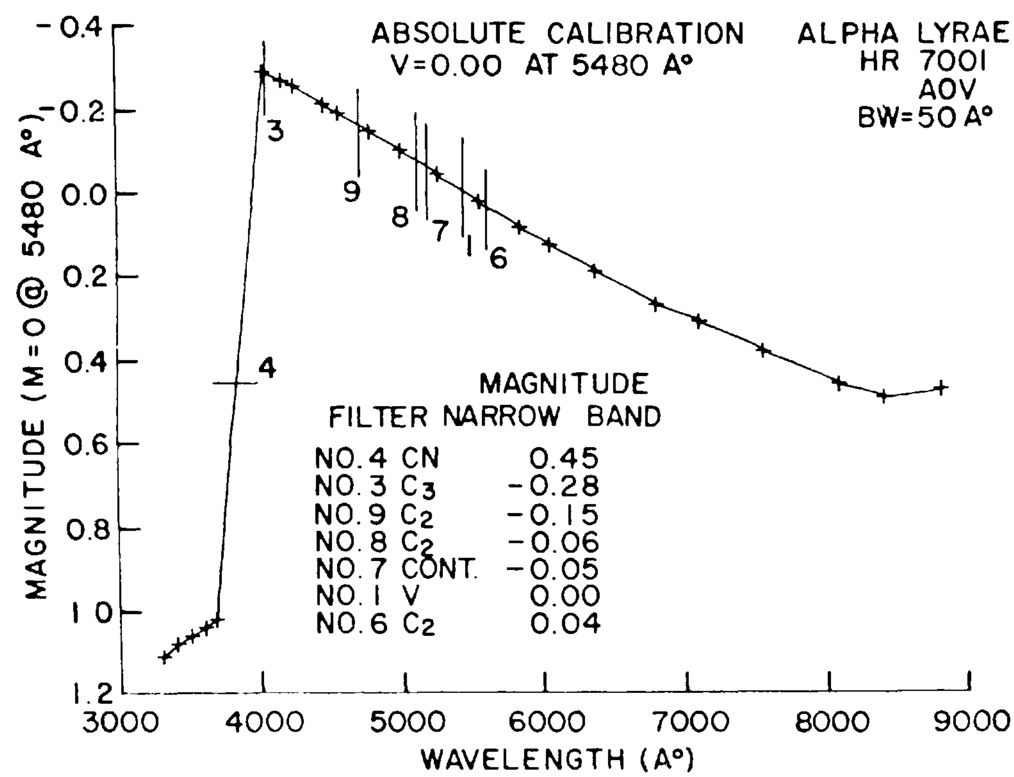

Figure 2 - Example of the determination of the narrow band magnitude scale for each filter from narrow band spectrophotometric scanner data.

https://doi.org/10.1017/S0252921100500761 Published online by Cambridge University Press

V. ERRORS

The least-squares technique by which the magnitude scale was derived can be characterized by three free parameters: the zero intercept, the relative scale, and the extinction correction. These errors are listed in Table VI. For the CN molecular line (filter #4), the error is considerably higher than shown due to the filter wavelength falling on the area of the spectrum containing the Balmer jump. Additional data errors arise from converting to a narrow band magnitude system. These systems were converted to absolute flux through the measurements of Oke and Schild (1970) of the star alpha Lyrae (figure 2). The total error of the comet measurements is then the combination of all these individual errors.

TABLE VI

Data Errors (Magnitudes)

	Filter	#4*	#3	#9	#8	#7	#1	#6
Standard Stars		$\pm 0^{m}.06$	0.05	0.05	0.03	0.05	0.02	0.02
α LYR		±0.02	0.02	0.02	0.02	0.02	0.02	0.02
<ext. °X>	Max.	±0.15	0.23	0.19	0.11	0.12	0.26	0.12
	Min.	±0.04	0.06	0.09	0.05	0.04	0.05	0.04
Relative Scale		±0.05	0.10	0.21	0.11	0.11	0.16	0.11
Zero Point		±0.22	0.25	0.45	0.21	0.22	0.23	0.23
Total	(Max.)	$\pm 0^{m}.28$	$\pm 0^{m}.36$	$\pm 0^{m}.53$	$\pm 0^{m}.26$	$\pm 0^{m}.28$	$\pm 0^{m}.38$	$\pm 0^{m}.28$

*Error is larger than table due to Balmer jump

VI. RESULTS

Good quality data were obtained on 13 days between November 1973 and February 1974 for all filters and most of the diaphragms. Table VII is a tabulation of these observations normalized to a distance of 1 A.U. by assuming an inverse-square distance dependence. On 1 December (2442018.0 J.D.) a small flare was observed to occur for all molecular lines and for the 5200 A° continuum (figure 3), although the increase was small for the CN filter (figure 4). This flare was followed on 4 December (2442021.0 J.D.) by a decrease in intensity which exceeded that expected from pre-flare conditions. For the inner regions of the coma (≤48" or ≤2.3×10^4 km) the 5200 A° continuum shows an unexpectedly low intensity on 23 November (figure 5, 2442010.0 J.D.). This effect is noticeable also in figure 3 for the larger diaphragm opening of 100" (4.1×10^4 km). In the outer coma a CN flare (3879 A°) was observed on 13 January (figure 4, 2442060.5 J.D.). Although fairly large in intensity, some uncertainty must be attached to this observation as it was made in the twilight sky overlooking Washington. On 28 January (2442075.5 J.D.) the visual filter (5454 A°) apparently responded to an increase in intensity within its large 235 A° bandwidth (figure 6). The reality of this increase is supported by the small increase in two nearby filters at 5165 A° and 5200 A°. At the same time there was also an increase for C_3 at 4057 A° (figure 3).

https://doi.org/10.1017/S0252921100500761 Published online by Cambridge University Press

TABLE VII

Magnitude (Normalized to 1 AU)

Diaphragm #1 9"

Day (J.D.) \ Filter	#4	#3	#9	#8	#7	#1	#6
2441990.9	-	-	-	-	-	-	-
2442010.0	9.4	-	11.7	10.4	-	-	10.0
2442016.9	8.6	12.1	11.0	9.6	11.0	11.6	9.7
2442018.0	8.6	-	10.7	9.3	10.4	11.3	9.0
2442021.0	-	-	12.1	9.6	11.4	11.9	10.1
2442060.5	8.0	11.4	10.0	8.4	11.9	10.9	9.3
2442061.5	8.1	11.5	10.6	8.9	11.3	10.8	9.8
2442069.5	9.9	12.2	12.0	10.7	12.7	13.1	10.1
2442075.5	10.0	-	13.0	11.2	-	-	11.5
2442080.6	10.8	-	-	11.8	-	-	-
2442094.6	-	-	-	-	-	-	-
2442096.6	-	-	-	-	-	-	-
2442099.6	-	-	-	-	-	-	-

Diaphragm #2 14"

Day (J.D.) \ Filter	#4	#3	#9	#8	#7	#1	#6
2441990.9	-	-	-	10.5	-	-	-
2442010.0	8.8	-	11.6	10.4	-	11.7	9.3
2442016.9	7.7	11.4	9.9	8.7	10.0	10.9	9.1
2442018.0	7.5	12.1	9.7	8.3	9.8	9.8	8.6
2442021.0	8.1	-	11.1	8.7	10.7	10.8	9.1
2442060.5	7.4	10.0	9.1	7.6	10.7	9.4	8.8
2442061.5	7.5	10.4	9.6	8.0	10.4	9.9	8.9
2442069.5	9.0	12.2	11.0	9.9	11.7	12.3	9.9
2442075.5	9.2	12.1	11.7	10.3	12.1	12.2	11.1
2442080.6	9.9	-	12.6	11.3	-	-	11.6
2442094.6	11.1	-	-	-	-	-	-
2442096.6	-	-	-	-	-	-	-
2442099.6	-	-	-	-	-	-	-

https://doi.org/10.1017/S0252921100500761 Published online by Cambridge University Press

TABLE VII (cont.)

Diaphragm #3 36"

Filter / Day (J.D.)	#4	#3	#9	#8	#7	#1	#6
2441990.9	-	10.6	11.0	9.5	-	11.1	-
2442010.0	6.5	9.6	8.6	8.0	-	8.8	7.7
2442016.9	5.8	8.8	7.7	6.6	8.3	8.3	7.3
2442018.0	5.7	8.1	6.9	5.8	7.9	7.0	6.8
2442021.0	6.1	9.2	8.3	6.4	8.1	8.1	7.0
2442060.5	5.6	8.2	6.9	5.7	8.2	7.1	6.8
2442061.5	5.6	8.2	7.1	5.8	8.2	7.6	7.1
2442069.5	7.1	9.3	8.8	7.4	9.7	9.4	8.5
2442075.5	7.4	9.8	9.4	8.1	10.3	9.7	9.1
2442080.6	8.1	10.7	10.3	9.0	11.0	11.2	9.8
2442094.6	9.2	12.1	11.7	10.4	-	-	-
2442096.6	9.2	-	12.2	10.7	-	-	-
2442099.6	10.5	-	-	11.2	-	-	-

Diaphragm #4 48"

Filter / Day (J.D.)	#4	#3	#9	#8	#7	#1	#6
2441990.9	-	-	10.1	9.0	9.6	10.4	8.4
2442010.0	6.0	9.0	7.9	6.6	10.7	8.2	7.3
2442016.9	5.3	8.2	7.1	6.2	7.9	7.8	6.9
2442018.0	5.1	7.6	6.4	5.3	7.1	6.7	6.3
2442021.0	5.6	8.7	7.7	6.0	7.7	7.7	6.7
2442060.5	5.3	8.0	6.4	5.3	7.7	6.7	6.5
2442061.5	5.1	7.8	6.6	5.4	7.7	6.7	6.6
2442069.5	6.5	9.0	8.1	6.9	9.3	8.8	8.0
2442075.5	7.0	9.4	8.8	7.5	9.8	9.2	8.7
2442080.6	7.6	10.3	9.8	8.5	10.7	10.7	9.6
2442094.6	8.6	11.7	10.9	9.7	11.3	-	10.2
2442096.6	8.8	11.7	11.6	10.2	11.6	-	10.6
2442099.6	10.1	-	-	10.7	-	-	-

https://doi.org/10.1017/S0252921100500761 Published online by Cambridge University Press

TABLE VII (cont.)

Diaphgram #5 100"

Day (J.D.) / Filter	#4	#3	#9	#8	#7	#1	#6
2441990.9	6.8	9.5	8.8	7.7	9.0	9.6	8.2
2442010.0	4.9	7.9	6.6	5.6	8.2	6.8	6.4
2442016.9	4.3	7.6	6.0	5.0	7.2	6.5	6.0
2442018.0	4.0	7.0	5.7	4.3	6.3	5.6	5.6
2442021.0	4.6	8.1	6.7	5.2	7.0	6.5	6.0
2442060.5	4.2	7.7	5.6	4.6	6.9	6.0	5.7
2442061.5	4.2	7.3	5.6	4.4	6.9	5.8	5.8
2442069.5	5.4	8.5	6.9	5.9	8.3	7.7	7.0
2442075.5	6.0	8.6	7.9	6.4	8.8	7.5	7.7
2442080.6	6.6	9.3	8.5	7.2	9.7	9.4	8.3
2442094.6	7.5	10.5	9.6	8.3	10.4	10.8	9.1
2442096.6	7.6	10.5	10.4	8.8	10.5	11.0	9.2
2442099.6	8.5	-	-	9.2	10.9	11.7	9.8

Diaphgram #6 220"

Day (J.D.) / Filter	#4	#3	#9	#8	#7	#1	#6
2441990.9	6.4	-	8.4	7.0	8.4	-	7.8
2442010.0	4.2	7.9	6.2	5.6	7.3	6.3	6.0
2442016.9	3.5	7.4	5.3	4.4	6.7	6.1	5.5
2442018.0	3.4	6.6	4.9	3.8	5.9	5.0	5.6
2442021.0	4.1	7.8	6.0	4.6	6.5	6.0	6.0
2442060.5	2.0	7.4	5.2	4.3	6.4	5.9	5.4
2442061.5	3.8	7.3	5.3	4.2	6.4	5.7	5.4
2442069.5	4.9	8.0	6.3	5.2	7.7	7.5	6.5
2442075.5	5.5	8.3	6.8	5.7	8.2	6.1	7.5
2442080.6	6.0	8.7	7.8	6.4	8.9	8.7	7.6
2442094.6	6.7	9.7	8.6	7.4	9.6	9.9	8.3
2442096.6	6.8	9.7	9.4	7.7	9.6	10.2	8.2
2442099.6	7.3	10.4	-	8.3	10.0	10.7	8.9

https://doi.org/10.1017/S0252921100500761 Published online by Cambridge University Press

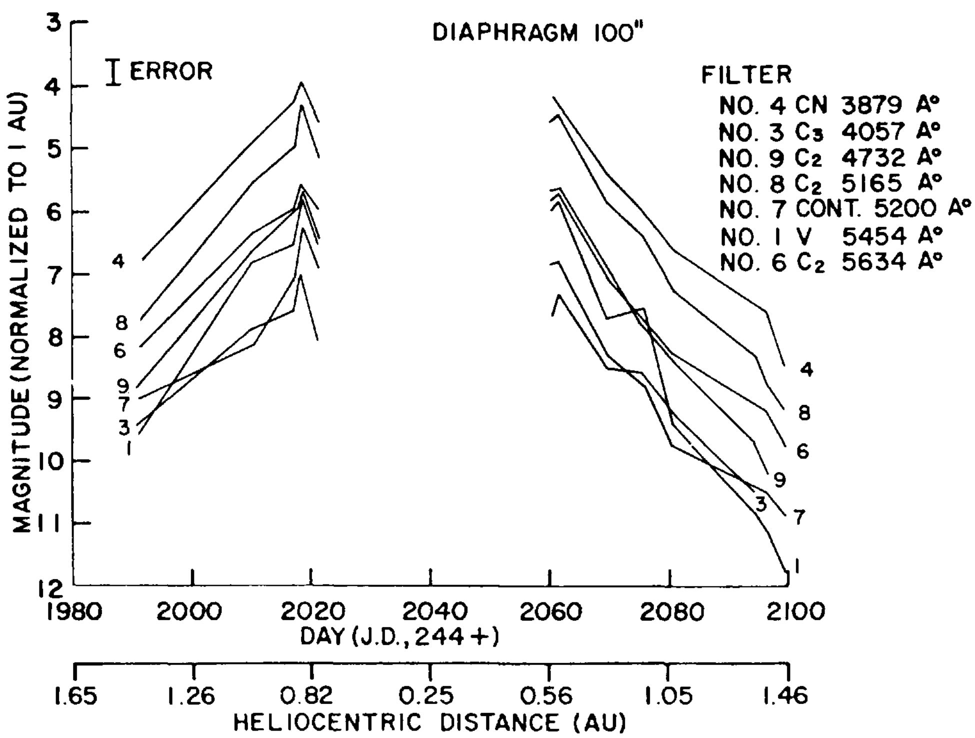

Figure 3 - Variation of comet magnitude (normalized to 1 A.U.) with heliocentric distance for each filter for the 100" diaphragm.

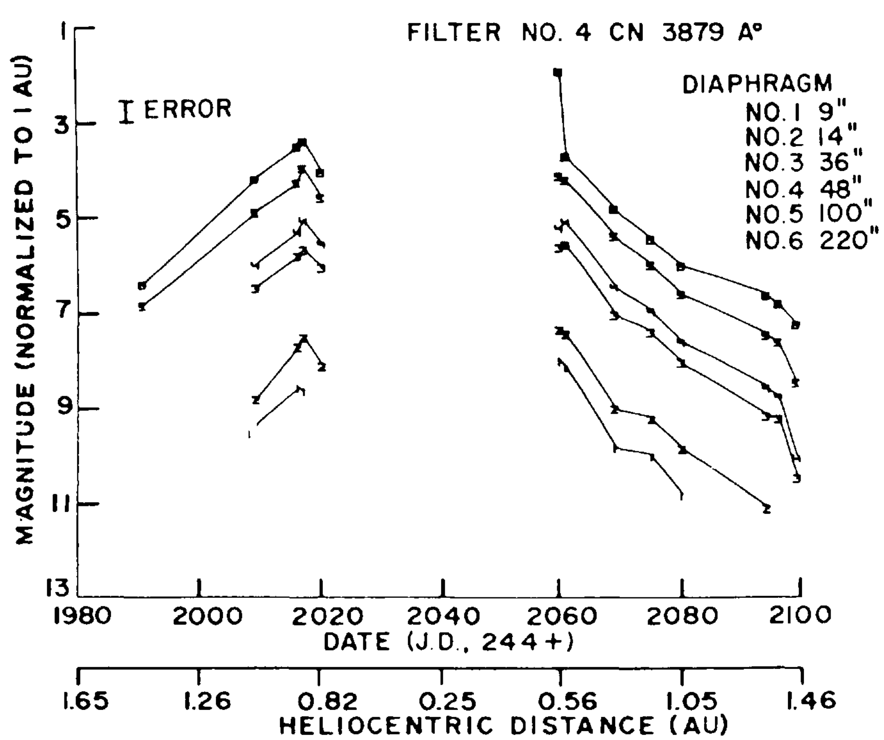

Figure 4 - Variation of comet magnitude (normalized to 1 A.U.) with heliocentric distance for the CN molecular for each diaphragm.

https://doi.org/10.1017/S0252921100500761 Published online by Cambridge University Press

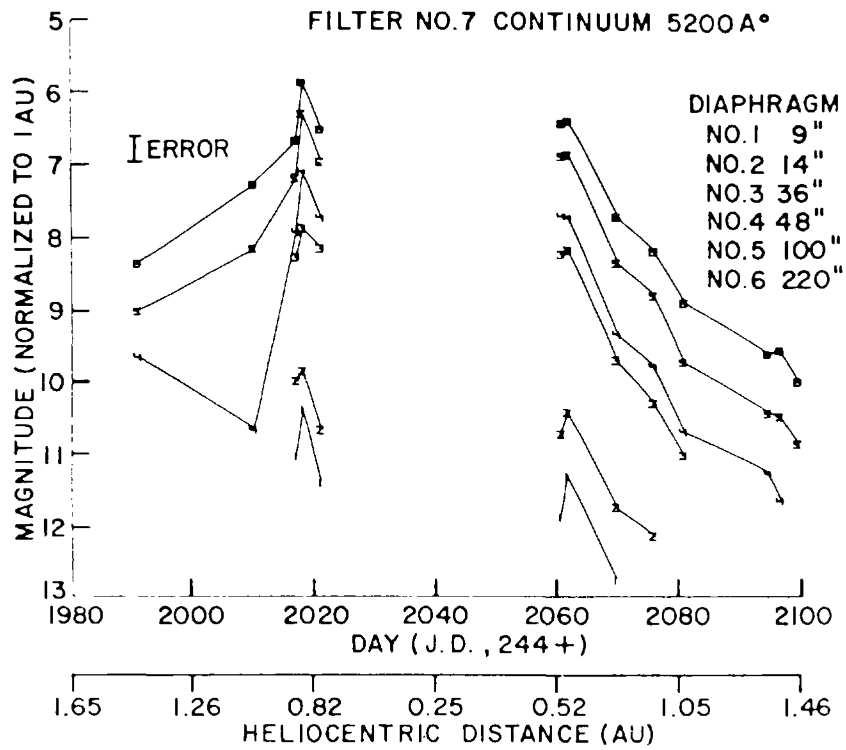

Figure 5 - Variation of comet magnitude (normalized to 1 A.U.) with heliocentric distance for the 5200 A° continuum for each diaphragm.

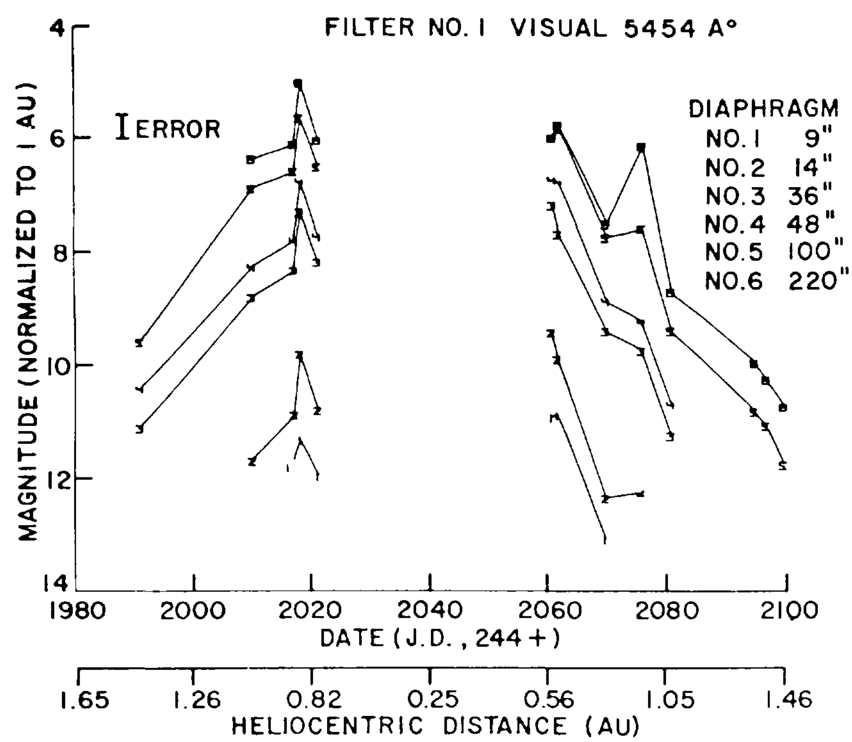

Figure 6 - Variation of comet magnitude (normalized to 1 A.U.) with heliocentric distance for the wide band visual (5454 A°) filter for each diaphragm.

The use of the six diaphragms allows a crude derivation of the radial dependence of the emission observed (assuming circular symmetry). The observed magnitude (m_i) at 1 A.U. inside a diaphragm (i) is related to the intensity, I_i (ergs sec^{-1} cm^{-2}) by

$$I_i = I_o\, 10^{-0.4\,(m_i - m_o)} , \qquad (1)$$

where I_o is the intensity for a magnitude m_o. If I_o is defined as the intensity which corresponds to a magnitude of zero, then equation (1) becomes

$$I_i = I_o\, 10^{-0.4\, m_i} . \qquad (2)$$

The surface brightness, S_i (ergs sec^{-1} cm^{-2} $sterad^{-1}$) can be related then to the intensity. In particular the surface brightness in the annulus between the radius (r_i) of the coma defined by diaphragm (i) and the radius (r_{i+1}) of diaphragm (i+1) is given by

$$S_{i+1,i} = I_o(10^{-m_{i+1}} - 10^{-m_i})/(\text{Area }(i+1) - \text{Area }(i)). \qquad (3)$$

Since the magnitude scale is based on the absolute flux of Alpha Lyrae, the value of I_o(for m = 0) has been taken as 3.64×10^{-9} $\Delta\lambda$ (ergs sec^{-1} cm^{-2}) as given by Oke and Schild (1970). The results are summarized in Table VIII. The average radii of the different annuli from the center of the coma are given in Table IX.

https://doi.org/10.1017/S0252921100500761 Published online by Cambridge University Press

TABLE VIII

Surface Brightness (ergs/sec-cm^2-sterad)

Filter #4 CN 3879 A°

Day (J.D.)	Diaphragm Δ(AU)	9"	14"	36"	48"	100"	220"
2441990.9	2.01	-	-	-	-	-	8.6×10^{-4}
2442010.0	1.53	8.4×10^{-2}	4.4×10^{-2}	7.8×10^{-2}	5.7×10^{-2}	3.5×10^{-2}	1.0×10^{-2}
2442016.9	1.38	1.8×10^{-1}	1.6×10^{-1}	1.4×10^{-1}	1.1×10^{-1}	5.8×10^{-2}	2.1×10^{-2}
2442018.0	1.36	1.8×10^{-1}	2.2×10^{-1}	1.5×10^{-1}	1.5×10^{-1}	8.1×10^{-2}	1.9×10^{-2}
2442021.0	1.31	-	-	1.1×10^{-1}	8.2×10^{-2}	4.4×10^{-2}	8.6×10^{-3}
2442060.5	0.81	3.0×10^{-1}	1.6×10^{-1}	1.7×10^{-1}	7.1×10^{-2}	6.8×10^{-2}	1.4×10^{-1}
2442061.5	0.81	2.8×10^{-1}	1.4×10^{-1}	1.7×10^{-1}	1.3×10^{-1}	6.0×10^{-2}	9.5×10^{-3}
2442069.5	0.84	5.3×10^{-2}	4.8×10^{-2}	4.2×10^{-2}	4.1×10^{-2}	2.2×10^{-2}	4.1×10^{-3}
2442075.5	0.93	4.8×10^{-2}	3.7×10^{-2}	3.2×10^{-2}	1.9×10^{-2}	1.2×10^{-2}	2.4×10^{-3}
2442080.6	1.02	2.3×10^{-2}	2.1×10^{-2}	1.7×10^{-2}	1.3×10^{-2}	7.0×10^{-2}	1.7×10^{-3}
2442094.6	1.36	-	-	6.1×10^{-3}	6.0×10^{-3}	3.2×10^{-3}	1.1×10^{-3}
2442096.6	1.41	-	-	-	3.6×10^{-3}	3.1×10^{-3}	1.0×10^{-3}
2442099.6	1.50	-	-	-	1.1×10^{-3}	1.6×10^{-3}	8.2×10^{-4}

Filter #3 C_3 4057 A°

Day (J.D.)	Diaphragm Δ(AU)	9"	14"	36"	48"	100"	220"
2441990.9	2.01	-	-	-	-	-	-
2442010.0	1.53	-	-	-	6.1×10^{-3}	3.3×10^{-3}	-
2442016.9	1.38	1.0×10^{-2}	6.6×10^{-3}	1.4×10^{-2}	1.3×10^{-2}	2.9×10^{-3}	2.8×10^{-4}
2442018.0	1.36	-	-	2.9×10^{-2}	1.9×10^{-2}	5.0×10^{-3}	1.1×10^{-3}
2442021.0	1.31	-	-	-	7.0×10^{-3}	1.8×10^{-3}	2.8×10^{-4}
2442060.5	0.81	2.0×10^{-2}	3.6×10^{-2}	2.2×10^{-2}	6.1×10^{-3}	1.5×10^{-3}	4.0×10^{-4}
2442061.5	0.81	1.8×10^{-2}	2.2×10^{-2}	2.4×10^{-2}	1.3×10^{-2}	3.3×10^{-3}	-
2442069.5	0.84	9.4×10^{-3}	-	9.3×10^{-3}	3.5×10^{-3}	1.1×10^{-3}	3.5×10^{-4}
2442075.5	0.93	-	-	5.5×10^{-3}	3.1×10^{-3}	1.4×10^{-3}	1.7×10^{-4}
2442080.6	1.02	-	-	-	1.3×10^{-3}	8.6×10^{-4}	2.1×10^{-4}
2442094.6	1.36	-	-	-	3.7×10^{-4}	3.2×10^{-4}	1.0×10^{-4}
2442096.6	1.41	-	-	-	-	3.2×10^{-4}	1.0×10^{-4}
2442099.6	1.50	-	-	-	-	-	-

Filter #9 C_2 4732 A°

Day (J.D.)	Diaphragm Δ(AU)	9"	14"	36"	48"	100"	220"
2441990.9	2.01	-	-	-	1.7×10^{-3}	9.2×10^{-4}	1.2×10^{-4}
2442010.0	1.53	8.6×10^{-3}	5.9×10^{-4}	1.0×10^{-2}	1.1×10^{-2}	7.0×10^{-3}	8.9×10^{-4}
2442016.9	1.38	1.6×10^{-2}	2.0×10^{-2}	2.2×10^{-2}	2.0×10^{-2}	1.1×10^{-2}	3.1×10^{-3}
2442018.0	1.36	2.2×10^{-2}	2.3×10^{-2}	4.9×10^{-2}	3.4×10^{-2}	1.1×10^{-2}	5.0×10^{-3}
2442021.0	1.31	6.0×10^{-3}	6.4×10^{-3}	1.4×10^{-2}	1.2×10^{-2}	5.5×10^{-3}	1.7×10^{-3}
2442060.5	0.81	4.1×10^{-2}	3.8×10^{-2}	4.6×10^{-2}	3.4×10^{-2}	1.3×10^{-2}	2.2×10^{-3}
2442061.5	0.81	2.4×10^{-2}	2.5×10^{-2}	4.0×10^{-2}	2.8×10^{-2}	1.5×10^{-2}	1.6×10^{-3}
2442069.5	0.84	6.6×10^{-3}	7.0×10^{-3}	8.0×10^{-3}	9.1×10^{-3}	5.1×10^{-3}	1.1×10^{-3}
2442075.5	0.93	2.6×10^{-3}	4.2×10^{-3}	4.7×10^{-3}	4.3×10^{-3}	1.7×10^{-3}	1.1×10^{-3}
2442080.6	1.02	-	-	2.0×10^{-3}	1.5×10^{-3}	1.2×10^{-3}	3.1×10^{-4}
2442094.6	1.36	-	-	-	7.6×10^{-4}	4.4×10^{-4}	1.9×10^{-4}
2442096.6	1.41	-	-	-	3.2×10^{-4}	2.0×10^{-4}	9.1×10^{-5}
2442099.6	1.50	-	-	-	-	-	-

Filter #8 C_2 5165 A°

Day (J.D.)	Diaphragm Δ(AU)	9"	14"	36"	48"	100"	220"
2441990.9	2.01	-	-	$2.7x10^{-3}$	$2.9x10^{-3}$	$2.3x10^{-3}$	$6.1x10^{-4}$
2442010.0	1.53	$2.7x10^{-2}$	-	$1.6x10^{-2}$	$5.1x10^{-2}$	$1.4x10^{-2}$	-
2442016.9	1.38	$5.5x10^{-2}$	$5.0x10^{-2}$	$5.5x10^{-2}$	$3.1x10^{-2}$	$2.7x10^{-2}$	$6.0x10^{-3}$
2442018.0	1.36	$7.3x10^{-2}$	$7.8x10^{-2}$	$1.2x10^{-1}$	$8.6x10^{-2}$	$4.6x10^{-2}$	$9.0x10^{-3}$
2442021.0	1.31	$5.5x10^{-2}$	$5.0x10^{-2}$	$6.8x10^{-2}$	$3.8x10^{-2}$	$1.8x10^{-2}$	$5.0x10^{-3}$
2442060.5	0.81	$1.7x10^{-1}$	$1.3x10^{-1}$	$1.2x10^{-1}$	$7.2x10^{-2}$	$2.8x10^{-2}$	$3.7x10^{-3}$
2442061.5	0.81	$1.1x10^{-1}$	$9.6x10^{-2}$	$1.2x10^{-1}$	$6.6x10^{-2}$	$4.2x10^{-2}$	$2.8x10^{-3}$
2442069.5	0.84	$2.0x10^{-2}$	$1.5x10^{-2}$	$2.8x10^{-2}$	$2.0x10^{-2}$	$1.1x10^{-2}$	$3.2x10^{-3}$
2442075.5	0.93	$1.3x10^{-2}$	$1.2x10^{-2}$	$1.4x10^{-2}$	$1.3x10^{-2}$	$7.1x10^{-3}$	$2.0x10^{-3}$
2442080.6	1.02	$7.3x10^{-3}$	$3.0x10^{-3}$	$6.2x10^{-3}$	$4.5x10^{-3}$	$3.7x10^{-3}$	$1.2x10^{-3}$
2442094.6	1.36	-	-	-	$1.9x10^{-3}$	$1.4x10^{-3}$	$8.9x10^{-4}$
2442096.6	1.41	-	-	-	$9.4x10^{-4}$	$1.4x10^{-3}$	$3.2x10^{-4}$
2442099.6	1.50	-	-	-	$6.0x10^{-4}$	$6.3x10^{-4}$	$2.2x10^{-4}$

Filter #6 C_2 5634 A°

Day (J.D.)	Diaphragm Δ(AU)	9"	14"	36"	48"	100"	220"
2441990.9	2.01	-	-	-	-	$3.6x10^{-4}$	$1.9x10^{-4}$
2442010.0	1.53	$3.8x10^{-2}$	$2.4x10^{-2}$	$1.8x10^{-2}$	$1.1x10^{-2}$	$6.3x10^{-3}$	$9.9x10^{-4}$
2442016.9	1.38	$5.0x10^{-2}$	$2.6x10^{-2}$	$2.7x10^{-2}$	$1.7x10^{-2}$	$9.0x10^{-3}$	$1.9x10^{-3}$
2442018.0	1.36	$9.6x10^{-2}$	$3.0x10^{-2}$	$4.3x10^{-2}$	$3.4x10^{-2}$	$1.1x10^{-2}$	-
2442021.0	1.31	$3.5x10^{-2}$	$3.7x10^{-2}$	$3.8x10^{-2}$	$1.6x10^{-2}$	$7.6x10^{-3}$	-
2442060.5	0.81	$7.3x10^{-2}$	$3.0x10^{-2}$	$4.5x10^{-2}$	$1.9x10^{-2}$	$1.1x10^{-2}$	$1.4x10^{-3}$
2442061.5	0.81	$4.6x10^{-2}$	$4.2x10^{-2}$	$3.3x10^{-2}$	$2.6x10^{-2}$	$1.0x10^{-2}$	$1.7x10^{-3}$
2442069.5	0.84	$3.5x10^{-2}$	$5.0x10^{-2}$	$8.1x10^{-3}$	$7.2x10^{-3}$	$3.8x10^{-3}$	$7.5x10^{-4}$
2442075.5	0.93	$9.6x10^{-3}$	$3.0x10^{-3}$	$5.4x10^{-3}$	$3.1x10^{-3}$	$2.0x10^{-3}$	$1.4x10^{-4}$
2442080.6	1.02	-	-	$2.7x10^{-3}$	$7.5x10^{-4}$	$1.3x10^{-3}$	$3.5x10^{-4}$
2442094.6	1.36	-	-	-	-	$5.9x10^{-4}$	$2.0x10^{-4}$
2442096.6	1.41	-	-	-	-	$6.1x10^{-4}$	$2.6x10^{-4}$
2442099.6	1.50	-	-	-	-	-	$1.3x10^{-4}$

Filter #7 Continuum 5200 A°

Day (J.D.)	Diaphragm Δ(AU)	9"	14"	36"	48"	100"	220"
2441990.9	2.01	-	-	-	-	$4.4x10^{-4}$	$1.5x10^{-4}$
2442010.0	1.53	-	-	-	-	$1.9x10^{-3}$	$5.6x10^{-4}$
2442016.9	1.38	$1.6x10^{-2}$	$1.7x10^{-2}$	$1.1x10^{-2}$	$6.7x10^{-3}$	$2.6x10^{-3}$	$6.3x10^{-4}$
2442018.0	1.36	$2.7x10^{-2}$	$1.4x10^{-2}$	$1.6x10^{-2}$	$2.4x10^{-2}$	$6.5x10^{-3}$	$1.1x10^{-3}$
2442021.0	1.31	$1.1x10^{-2}$	$6.9x10^{-3}$	$1.5x10^{-2}$	$8.0x10^{-3}$	$3.1x10^{-3}$	$7.6x10^{-4}$
2442060.5	0.81	$6.8x10^{-3}$	$9.6x10^{-3}$	$1.4x10^{-2}$	$9.6x10^{-3}$	$3.7x10^{-3}$	$8.4x10^{-4}$
2442061.5	0.81	$1.2x10^{-2}$	$1.1x10^{-2}$	$1.3x10^{-2}$	$9.6x10^{-3}$	$3.7x10^{-3}$	$8.4x10^{-4}$
2442069.5	0.84	$3.2x10^{-3}$	$3.5x10^{-3}$	$3.2x10^{-3}$	$1.8x10^{-3}$	$1.2x10^{-3}$	$2.9x10^{-4}$
2442075.5	0.93	-	-	$1.8x10^{-3}$	$1.4x10^{-3}$	$7.5x10^{-4}$	$1.8x10^{-4}$
2442080.6	1.02	-	-	-	$4.0x10^{-4}$	$3.3x10^{-4}$	$1.2x10^{-4}$
2442094.6	1.36	-	-	-	-	$1.6x10^{-4}$	$6.2x10^{-5}$
2442096.6	1.41	-	-	-	-	$1.7x10^{-4}$	$6.7x10^{-5}$
2442099.6	1.50	-	-	-	-	$1.4x10^{-4}$	$4.6x10^{-5}$

https://doi.org/10.1017/S0252921100500761 Published online by Cambridge University Press

Filter #1 Visual 5454 A°

Day (J.D.)	Diaphragam Δ(AU)	9"	14"	36"	48"	100"	220"
2441990.9	2.01	-	-	-	$4.8x10^{-3}$	$1.4x10^{-3}$	-
2442010.0	1.53	-	-	$3.7x10^{-2}$	$3.2x10^{-2}$	$2.6x10^{-2}$	$4.2x10^{-3}$
2442016.9	1.38	$4.1x10^{-2}$	$2.6x10^{-2}$	$5.8x10^{-2}$	$4.0x10^{-2}$	$3.3x10^{-2}$	$4.2x10^{-3}$
2442018.0	1.36	$5.4x10^{-2}$	$1.1x10^{-1}$	$1.4x10^{-1}$	$1.3x10^{-1}$	$6.9x10^{-2}$	$1.6x10^{-2}$
2442021.0	1.31	$3.1x10^{-2}$	$3.9x10^{-2}$	$7.0x10^{-2}$	$3.7x10^{-2}$	$3.2x10^{-2}$	$5.6x10^{-3}$
2442060.5	0.81	$7.9x10^{-2}$	$1.7x10^{-1}$	$1.7x10^{-1}$	$9.3x10^{-2}$	$3.6x10^{-2}$	$1.5x10^{-3}$
2442061.5	0.81	$8.6x10^{-2}$	$7.8x10^{-1}$	$1.1x10^{-1}$	$1.7x10^{-1}$	$5.1x10^{-2}$	$1.8x10^{-3}$
2442069.5	0.84	$1.0x10^{-2}$	$7.9x10^{-3}$	$2.1x10^{-2}$	$1.9x10^{-2}$	$1.0x10^{-2}$	$6.4x10^{-4}$
2442075.5	0.93	-	-	$1.6x10^{-2}$	$1.1x10^{-2}$	$1.5x10^{-2}$	$1.0x10^{-2}$
2442080.6	1.02	-	-	-	$2.8x10^{-3}$	$2.3x10^{-3}$	$6.0x10^{-4}$
2442094.6	1.36	-	-	-	-	-	$2.3x10^{-4}$
2442096.6	1.41	-	-	-	-	-	$1.6x10^{-4}$
2442099.6	1.50	-	-	-	-	-	$1.2x10^{-4}$

TABLE IX.

Radius (km) at which Table VIII Surface Brightness is Calculated

Day (J.D.)	Diaphragm Δ(AU)	9"	14"	36"	48"	100"	220"
2441990.9	2.01	-	-	$1.8x10^4$	$3.1x10^4$	$5.4x10^4$	$1.2x10^5$
2442010.0	1.53	$2.5x10^3$	$6.4x10^3$	$1.4x10^4$	$2.3x10^4$	$4.1x10^4$	$8.9x10^4$
2442016.9	1.38	$2.3x10^3$	$5.8x10^3$	$1.3x10^4$	$2.1x10^4$	$3.7x10^4$	$8.0x10^4$
2442018.0	1.36	$2.2x10^3$	$5.7x10^3$	$1.2x10^4$	$2.1x10^4$	$3.7x10^4$	$7.9x10^4$
2442021.0	1.31	$2.1x10^3$	$5.5x10^3$	$1.2x10^4$	$2.0x10^4$	$3.5x10^4$	$7.6x10^4$
2442060.5	0.81	$1.3x10^3$	$3.4x10^3$	$7.3x10^3$	$1.2x10^4$	$2.2x10^4$	$4.7x10^4$
2442061.5	0.81	$1.3x10^3$	$3.4x10^3$	$7.3x10^3$	$1.2x10^4$	$2.2x10^4$	$4.7x10^4$
2442069.5	0.84	$1.4x10^3$	$3.5x10^3$	$7.6x10^3$	$1.3x10^4$	$2.3x10^4$	$4.9x10^4$
2442075.5	0.93	$1.5x10^3$	$3.9x10^3$	$8.4x10^3$	$1.4x10^4$	$2.5x10^4$	$5.4x10^4$
2442080.6	1.02	$1.7x10^3$	$4.3x10^3$	$9.3x10^3$	$1.6x10^4$	$2.7x10^4$	$5.9x10^4$
2442094.6	1.36	-	-	-	$2.1x10^4$	$3.7x10^4$	$7.9x10^4$
2442096.6	1.41	-	-	-	$2.2x10^4$	$3.8x10^4$	$8.2x10^4$
2442099.6	1.50	-	-	-	$2.3x10^4$	$4.0x10^4$	$8.7x10^4$

https://doi.org/10.1017/S0252921100500761 Published online by Cambridge University Press

In summary, photometric observations of the coma of comet Kohoutek (1973f) were made at the Cassegrain focus of a 36-inch telescope. The observations consisted of one wide (visual, 5454 A°) and six narrow (CN,3879 A°; C_3, 4057 A°; C_2, 4732 A°, 5165 A°, 5634 A°; continuum, 5200 A°) band interference filters. In addition each filter was used with six diaphragms (9,14,36,48,100,220"). Good quality data were obtained on 13 days between November 1973 and February 1974. A small flare was observed on 1 December for all filters, a CN flare on 13 January, and a visual flare on 28 January. The data have been reduced to absolute narrow band magnitudes of the comet for the 13 days. The radial dependence of the surface brightness has been derived from the set of diaphragms and future work will be directed toward using these results for modeling density distributions for the coma.

The author would like to thank C. McCracken, P. Taylor, T. Parker and C. Lowe for their valued assistance.

https://doi.org/10.1017/S0252921100500761 Published online by Cambridge University Press

REFERENCES

Breger, M., 1971, Communications in Astronomy From Stony Brook, #1.

Iriarte, B., Johnson, H.L., Mitchell, R.I., and Wisniewski, W., 1965, Sky and Telescope, 30, 24.

Oke, J.B. and Schild, R.E., 1970, Astrophysical Journal, 161, 1015.